

# Time-domain estimation of acoustic radiation modes and active structural acoustic control

Khairul A. M. Nor<sup>1,2</sup>, Brian R. Mace<sup>1</sup> and Yusuke Hioka<sup>1</sup>

<sup>1</sup> Department of Mechanical Engineering,  
The University of Auckland, Auckland 1142, New Zealand  
Email: [kmdn813@aucklanduni.ac.nz](mailto:kmdn813@aucklanduni.ac.nz)

<sup>2</sup> Department of Mechatronics Engineering,  
International Islamic University Malaysia, 53100 Kuala Lumpur, Malaysia

## ABSTRACT

This paper presents a method of calculating the radiated sound power of vibrating structures based on the time domain estimation of acoustic radiation modes (ARMs). Each ARM is frequency-dependent, radiates power independent of the other ARMs and can be estimated in the time domain from measurements made at discrete sensor locations on the surface of the radiating structure. The individual ARM components are estimated digitally in the time domain using finite impulse response filters, which are designed to provide a best weighted fit to the ARMs in the frequency domain. The ARM amplitudes are estimated by filtering the vectors of measured velocities at points on the radiating surface with these ARM filters, before summing the product of the square of these amplitudes with the relevant eigenvalues to estimate the radiated sound power. The method is described with reference to a simply supported beam model. The results show that the sound power calculated from the proposed approach and from a frequency domain approach are comparable. Finally, a time domain feedforward active structural acoustic control system developed using the proposed method is presented and time domain simulations demonstrate the performance of the system.

## 1. INTRODUCTION

Advances in sensor, actuator and microprocessor technologies nowadays provide more possibilities for noise control, namely active noise control (ANC) and active structural acoustic control (ASAC). ANC uses secondary sources to generate a sound signal which has an equal magnitude and is 180 degrees out of phase with the unwanted noise signal, in order to cancel that noise (Elliott & Nelson 1990; Kuo & Morgan 1999; Qiu & Ji 2010). Although it is a particularly efficient tool for 1-dimensional noise problems, ANC systems become increasingly complicated and uneconomical, with the number of secondary loudspeakers rising in proportion to the cube of the excitation frequency in a 3-dimensional enclosure (Elliott 1994). The ASAC method however can reduce this complexity to a 2-dimensional problem by controlling the vibration of the surface of a structure to suppress the radiated noise. This uses a smaller number of structural actuators to produce global far-field attenuation as compared to ANC (Clark & Fuller 1991; Fuller et al. 1996; Pan & Bao 1998; Carneal & Fuller 2004).

A number of approaches to ASAC methods have been developed. For instance, Pinte et al. (2009) proposed iterative learning control for active control of repetitive impact noise. The approaches of vibro-acoustic modes were proposed to control both sound and vibration simultaneously (Grewal et al. 2000; Palumbo et al. 2001; Kaizuka & Tanaka 2008). Bianchi et al. (2004), and Gardonio et al. (2004a, 2004b) developed a sound radiation control system using direct velocity feedback (DVF) with a configuration of collocated accelerometers and piezoelectric patches. Sound radiation from structural vibration modes was decoupled by investigating the acoustic radiation modes (ARMs) and radiation modal expansion before application to practical real-time control (Currey & Cunefare 1995; Gibbs et al. 2000). Volume velocity control has proven to be an effective strategy to reduce overall sound radiation especially at low frequencies, since the first ARM accounts for the most sound energy radiation, and has a close relationship to the net volume velocity at low frequency (Johnson & Elliott 1995; Sors & Elliott 2002). With the identified model, the control system was designed according to a Hankel-Norm specification to suppress noise radiated from a vibrating structure (Choi 2006).

The accuracy of estimating the sound power is vital in ASAC. The sound power generated by a vibrating structure can be measured as a superposition of its ARMs, i.e. the velocity distributions that radiate power

independently to the acoustic far-field (Cunefare 1991; Elliott & Johnson 1993). These ARMs are physically basis vectors orthogonal to each other in vector space, and each basis vector represents a particular velocity pattern. The unique feature of ARMs is that they depend only on the radiator geometry and frequency. Thus, the far-field sound pressure and power can be estimated even without information of the mechanical properties and boundary conditions of the radiators (Elliott & Johnson 1993). Equally, by using actuators to reduce the corresponding distributed surface velocities that contribute to the, often few, ARMs with significant radiation efficiencies, the overall radiated sound power can be reduced considerably. However, one problem with ARM approaches is that the individual radiation mode shapes are frequency dependent, and that the radiation efficiency of each ARM is also frequency dependent. This frequency dependence introduces significant difficulties for broad-band, real-time control, and hence the majority of previous work concerns discrete frequency or frequency-domain methods. This paper however concerns a time domain approach for broad-band control.

Unlike frequency-domain approaches, time-domain estimation of ARMs enables a broader frequency range of approximation and thus reduces the controller dimensionality in ASAC system (Berkhoff 2002). However, few studies on time domain ARMs and the radiated sound power have been carried out. Among the earliest works on this is the Discrete Structural Acoustic Sensing (DSAS) technique by Maillard (1997). His work provides time domain estimates of the radiated far-field sound pressure. Arrays of FIR filters, whose impulse responses were constructed from the appropriate Green function, were employed to process the measured acceleration signals in the time domain. Berkhoff (2002) identified the ARMs by extracting the underlying Green function using a time-domain inverse filtering technique. The work of Wu (2009) managed to calculate the sound power using measured acceleration distribution instead of velocity distribution. However, none of them estimate the sound power from the time-domain estimates of the ARM itself.

This paper presents a method of calculating the radiated sound power of vibrating structures based on the time domain estimation of ARMs. A time domain ASAC system developed using the proposed method is also presented. The remainder of this paper is organized as follows. The theoretical background of acoustic radiation modes and the radiation efficiency are described in Section 2. The method of estimation of ARMs in the time domain using FIR filters is proposed in Section 3. Section 4 discusses the time domain estimation of the radiated sound power in ARM filters introduced in Section 3. Comparison between theoretical and time-domain simulated sound power is also made. Section 5 presents the implementation of feedforward ASAC strategy on a vibrating beam. Finally, section 6 concludes this paper.

## 2. THEORY

### 2.1 Acoustic radiation modes

The radiated sound power from the surface can be expressed in term of the ARMs of the surface using the elemental radiator formulation approach, which can be written in a vector-matrix form as (Elliott & Johnson 1993)

$$W = \mathbf{v}^H \mathbf{M} \mathbf{v}, \quad (1)$$

where  $W$  is the sound power, superscript  $H$  is the Hermitian transpose,  $\mathbf{v}$  is the velocity vector whose entries are the elemental velocities. The radiation resistance matrix  $\mathbf{M}$  can be decomposed into

$$\mathbf{M} = \mathbf{Q} \mathbf{\Lambda} \mathbf{Q}^T, \quad (2)$$

where the superscript  $T$  is the transpose,  $\mathbf{\Lambda}$  is a diagonal matrix of real and positive eigenvalues,  $\lambda_r$ , and  $\mathbf{Q}$  is a matrix whose columns are the orthogonal eigenvectors of matrix  $\mathbf{M}$ . Each eigenvector in matrix  $\mathbf{Q}$  represents a possible velocity pattern of the surface, which is also known as an acoustic radiation mode (ARM). The  $r^{th}$  ARM amplitude  $y_r$  is the product of the  $r^{th}$  eigenvector of matrix  $\mathbf{Q}$ ,  $\mathbf{Q}_r$ , and the velocity vector  $\mathbf{v}$ , i.e.

$$y_r = \mathbf{Q}_r^T \mathbf{v}, \quad (3)$$

These ARM amplitudes are functions of position and frequency only but not boundary conditions, hence are not dependent on the natural modes of the structure. The total radiated acoustic power can then be re-written in the form

$$W = \mathbf{y}^H \Lambda \mathbf{y} = \sum_{r=1}^R |y_r|^2 \lambda_r. \tag{4}$$

The radiation efficiency of the individual ARM is defined as (Mao & Pietrzko 2013)

$$\sigma_r = \frac{2N}{\rho_0 c_0 A} \lambda_r, \tag{5}$$

where  $\rho_0$  is the air density,  $c_0$  is the sound velocity in air,  $N$  is the total number of elemental radiators with equal area and  $A$  is the total surface area of the radiator. The ARMs are frequency-dependent and Equation (3) can be written in the frequency domain as

$$Y_r(\omega) = \mathbf{Q}_r(\omega)^T \mathbf{V}(\omega) = \sum_{n=1}^N Q_{r,n}(\omega) V_n(\omega), \tag{6}$$

where  $\omega$  is the angular frequency and  $Y_r(\omega)$  is the ARM amplitude in the frequency domain. In vector-matrix form, this becomes

$$\begin{Bmatrix} Y_1(\omega) \\ \vdots \\ Y_r(\omega) \\ \vdots \\ Y_R(\omega) \end{Bmatrix} = \begin{bmatrix} Q_{1,1}(\omega) & \cdots & Q_{1,n}(\omega) & \cdots & Q_{1,N}(\omega) \\ \vdots & \ddots & & & \vdots \\ Q_{r,1}(\omega) & & \ddots & & Q_{r,N}(\omega) \\ \vdots & & & \ddots & \vdots \\ Q_{R,1}(\omega) & \cdots & Q_{R,n}(\omega) & \cdots & Q_{R,N}(\omega) \end{bmatrix} \begin{Bmatrix} V_1(\omega) \\ \vdots \\ V_n(\omega) \\ \vdots \\ V_N(\omega) \end{Bmatrix}, \tag{7}$$

where  $Q_{r,n}(\omega)$  is the entry of vector  $\mathbf{Q}_r(\omega)$  for the  $r^{th}$  ARM and at the  $n^{th}$  element, and  $V_n(\omega)$  is the  $n^{th}$  element of vector  $\mathbf{V}(\omega)$ .

### 2.2 Numerical examples of ARMs

Numerical examples of the frequency-dependent ARMs and the radiation efficiencies are presented here. Figure 1 shows the first three ARM shapes of a one-dimensional radiating plane structure, e.g. a baffled beam, when excited in the frequency range of  $kl=0$  to  $kl=10$ , where  $kl$  is the dimensionless frequency,  $k=\omega/c_0$  is the wavenumber, and  $l$  is the length of the structure. At low frequencies, i.e.  $kl \leq 1$ , the velocity distributions for the first, second and third ARMs of a beam shown in Figure 1, are similar to a piston-like motion, a rocking motion and a quadratic velocity variation, respectively. As frequency increases, their shapes become more curved.

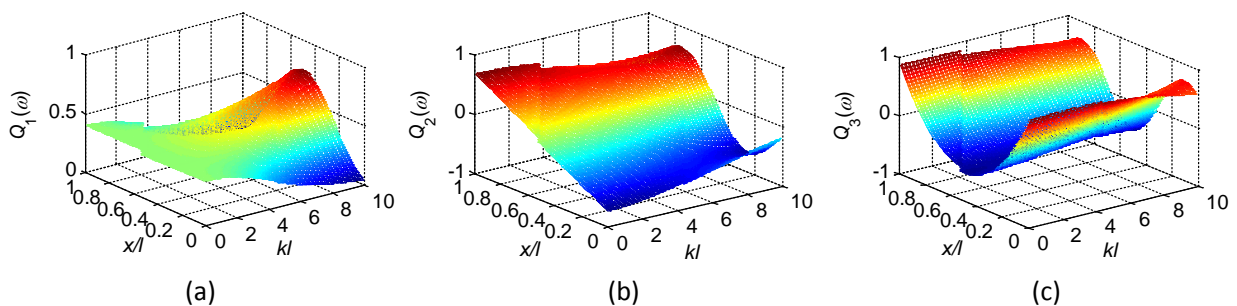


Figure 1: (a) First, (b) second and (c) third ARMs of one-dimensional baffled structure against position and dimensionless frequency  $kl$ .

Figure 2 shows the corresponding radiation efficiency of the first five ARMs of the beam which increase when frequency increases. It can be seen that the lower ARM orders are more efficient at low frequencies. This means, that significant attenuation of the total radiated sound power at low frequencies can be achieved by controlling the sound power of only the first few ARMs.

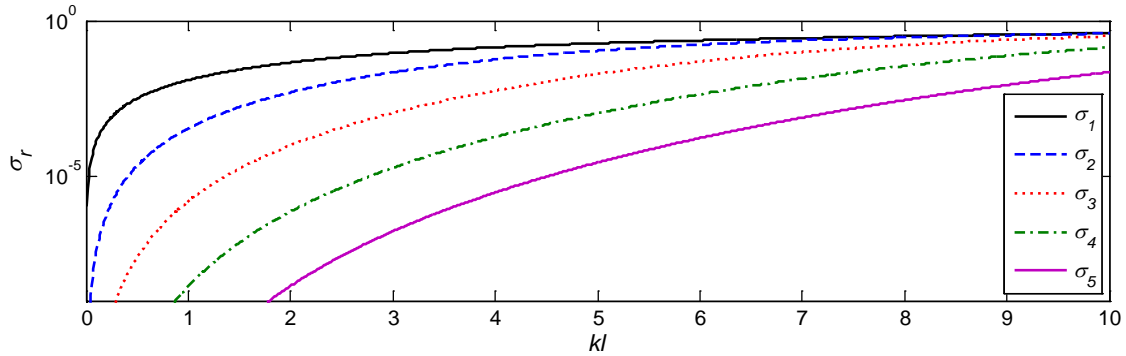


Figure 2: Radiation efficiencies of the first five ARMs

### 3. ACOUSTIC RADIATION MODE FILTERS

The ARM estimates are made by measuring responses at a number of discrete points on the radiating surface and then weighting and summing these point measurements. It is important to highlight that the ARM shapes are frequency dependent implying that the weights themselves must be frequency dependent as well. The time-domain ARM amplitude,  $y_r(t)$  is given by

$$y_r(t) \approx \sum_{n=1}^N q_{r,n}(t) * v_n(t), \tag{8}$$

where  $q_n(t)$  is the inverse Fourier transform and also the impulse response of a filter whose frequency response is  $Q_n(\omega)$  and  $v_n(t)$  is the inverse Fourier transform of  $V_n(\omega)$ . In digital applications, the ARMs are estimated at discrete times  $t=m\tau$  with a sampling frequency of  $f_s=1/\tau$ , hence Equation (8) becomes

$$y_r(m) = \sum_{n=1}^N \left\{ \sum_{s=0}^S q_{r,n}(s) v_n(m-s) \right\}, \tag{9}$$

where  $y_r(m)$  is the  $r^{th}$  ARM amplitude at time sample  $m$ .  $q_{r,n}(s)$  is the time sampled values of  $q_n(t)$  truncated to a sample length of  $S+1$ , thus it is regarded as the filter coefficients of a finite impulse response (FIR) filter which as applied to the velocity measurements  $v_n$  of each  $n$  velocity sensors.

This causal FIR filter in equation (9) will never be better than a non-causal filter that uses future values of  $v_k$ , i.e. for  $s < 0$ , because causality adds a constraint to the approximation. However, the non-causal filter is not practical for the purpose of real-time application. To make a non-causal yet practically feasible filter for a real-time implementation, a time-delay of  $d$  time steps is introduced (Mace & Halkyard 2000). This new filter will try to have a frequency response  $Q_{r,n}(\omega)\exp(-i\omega d/f_s)$  where  $i$  is the imaginary unit. This filter will produce an approximation of  $y_r(m)$  at time step  $m+d$  and at the same time is able to use  $(2d + 1)$  coefficients for the optimal estimation of  $Q_n(\omega)$  in the least square sense, i.e.

$$y_r(m) = \sum_{n=1}^N \left\{ \sum_{s=-d}^{s=d} q_{r,n}(s) v_n(m-s) \right\}, \tag{10}$$

For certain applications, providing an estimate  $d$  time steps later is not important, for example for the estimation of radiated sound power or use as an error function in adaptation schemes. For real-time control

applications the delay deteriorates the performance of the system, the issue being whether the non-causal, delayed filter of equation (10) perform better than the causal filter approximation of equation (9).

#### 4. NUMERICAL SIMULATIONS

This section demonstrates how the radiated sound power of a vibrating structure can be estimated in the time domain and realized using MATLAB/Simulink. The method is illustrated with reference to a baffled simply supported beam model with size 500 mm x 40 mm x 4 mm. Other parameters are given in Table 1. Here, the Matlab function *invfreqz* is used to calculate the filter coefficients of the FIR filters and the frequency response of the implemented filter is calculated using the function *freqz*.

Table 1: Parameters

Parameter	Value
Density of beam, $\rho$ (kg m <sup>-3</sup> )	7800
Young Modulus of beam, $E$ (GPa)	200
Modal damping ratio of beam, $\beta_p$	0.01
Density of air, $\rho_0$ (kg m <sup>-3</sup> )	1.239
Speed of sound in air, $c_0$ (m s <sup>-1</sup> )	340
Sampling frequency, $f_s$ (Hz)	1024

##### 4.1 Estimation of acoustic radiation modes

The ARMs filters, discussed in Section 3, are constructed in the time domain using 23<sup>rd</sup> order FIR filters with 11-step delay. These FIR filters are designed by a least-squares fit to the ideal frequency responses at 512 uniformly spaced frequencies up to the Nyquist frequency, i.e. 512 Hz with uniform weighting. Examples of the estimated frequency-dependent ARMs at  $x=325$  mm on the beam are illustrated in Figure 3. It can be seen that the magnitude is estimated very accurately while the phase is linear to a very good approximation, this representing the time delay.

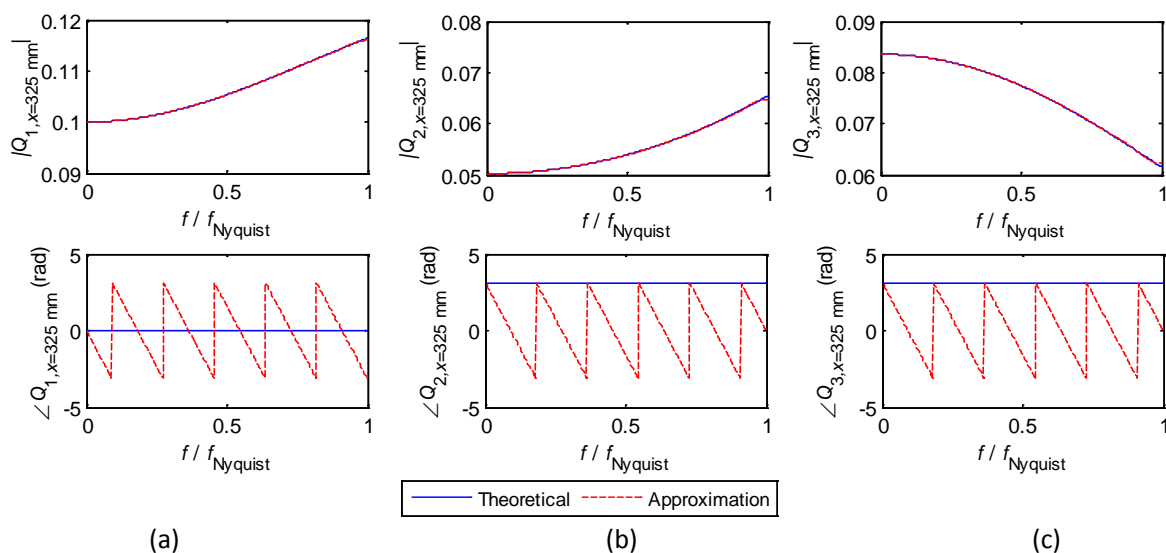


Figure 3: Estimation of (a) the first, (b) second and (c) third ARMs of the beam at  $x = 325$ mm using 23<sup>th</sup> order FIR filters with 11-step delay

##### 4.2 Time-domain estimation of the radiated sound power

Simulink is used to estimate the radiated sound power in real time. The primary source is a random point force,  $F_{pri}(t)$  (band-passed filtered using a 5<sup>th</sup> order elliptical filter with normalized edge frequencies of 0.1 and 0.9 of Nyquist frequency, 0.5 dB passband ripple and 20dB stopband attenuation) acts on the beam at  $x_0$ . The simulation duration is 10 seconds.

A total of ten sensors ( $N=10$ ), equally spaced on the radiating surface, are employed to measure the velocity distribution. The transfer function from the excitation point  $x_0$  to the  $n^{\text{th}}$  sensor located at  $x = x_n$  is defined as (Mao & Pietrzko 2013)

$$H_n(\omega) = \sum_{p=0}^{\infty} i\omega(\omega_p^2 - \omega^2 + 2i\beta_p\omega\omega_p)^{-1} \varphi_p(x_0)\varphi_p(x_n), \tag{11}$$

where  $p$  is the mode number,  $\omega_p$  is the  $p^{\text{th}}$  natural frequency of the beam and  $\varphi_p(x)$  is the mass normalized structural mode shape. The mode shapes for a simply supported beam are  $\varphi_p(x) = \sin(p\pi x/l)$ . These sensor transfer functions are then implemented in the time domain using 9<sup>th</sup> order infinite impulse response (IIR) filters.

Next, the time series of ARM amplitudes are measured by filtering the time series of the sensor outputs with the ARM filters developed in the previous section, before summing them. Note that each ARM amplitude requires a number  $N$  of ARM filters. The resulting time series are sampled with 50% overlapped Hanning-window to create 39 frames with 512 points in length and zero-padded with an additional 2048 points. Then the frequency-domain estimate of the ARM amplitude is obtained by finding the average of the discrete Fourier transform of these time series. Finally the radiated sound power is estimated by calculating the product of the square of these amplitudes with the corresponding eigenvalues. The block diagram representation of radiated sound power estimation is given in Figure 4.

Figure 5 shows the radiated sound power obtained using theoretical and time-domain estimation methods when the beam is excited by a point force at  $x_0 = 75$  mm. It is found that the radiated sound power estimated from the time domain ARM method is in good agreement with the theoretical value.

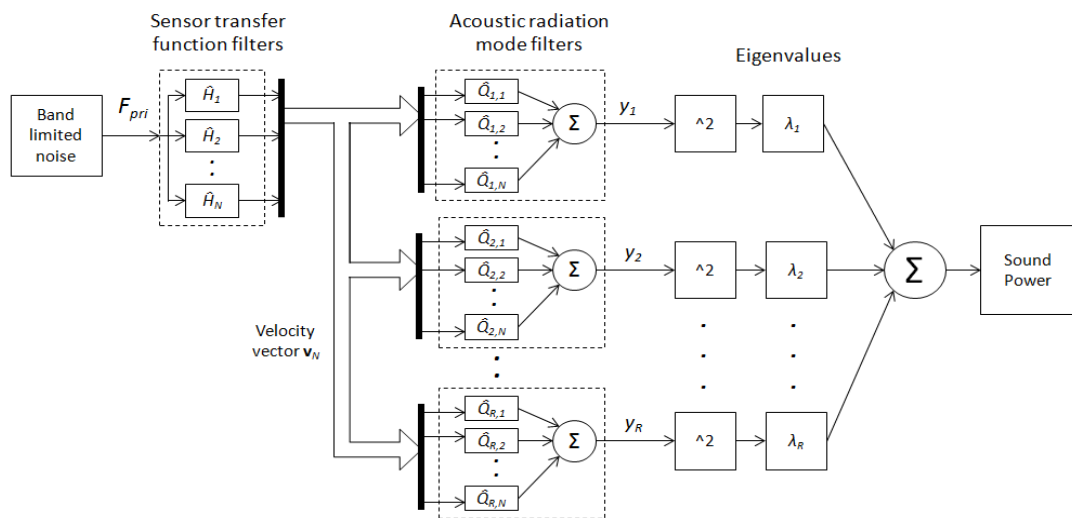


Figure 4: Block diagram representation of the time domain radiated sound power estimation

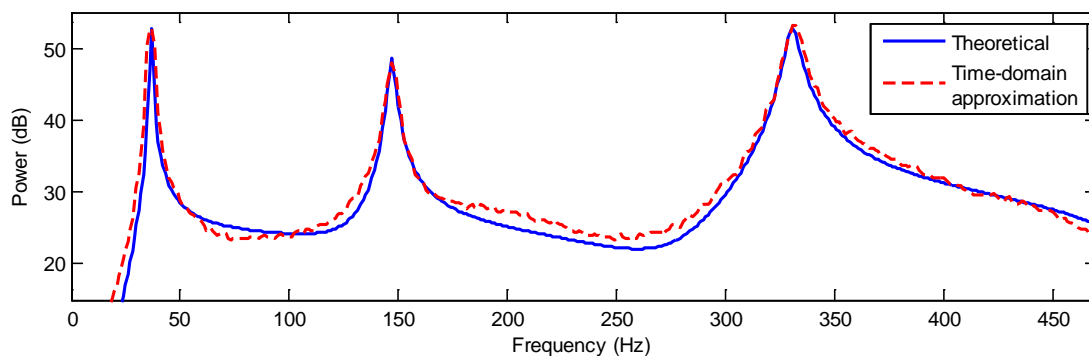


Figure 5: Estimation of radiated sound power for beam when the primary force located at  $x_0 = 75$  mm

### 5. FEEDFORWARD ACTIVE STRUCTURAL ACOUSTIC CONTROL

This section discusses the implementation of feedforward ASAC strategy on the vibrating beam. Theoretically, the sound power of the first  $j$  ARMs can be completely attenuated when the structure's velocity is orthogonal to the first  $j$  ARM vectors, i.e. the ARM amplitudes of the corresponding modes are zero (Mao & Pietrzko 2013). Mathematically it can be written as

$$\left[|Y_1(\omega)|, \dots, |Y_j(\omega)|\right]^T = \left[\mathbf{Q}_1(\omega), \dots, \mathbf{Q}_j(\omega)\right]^T \cdot \mathbf{V}(\omega) = \mathbf{0}. \tag{12}$$

The velocity can be divided into part caused by the primary and secondary forces,  $\mathbf{v}_{pri}$  and  $\mathbf{v}_{sec}$  respectively. Here

$$\mathbf{V}(\omega) = \mathbf{V}_{pri}(\omega) + \sum_j \mathbf{V}_{sec,j}(\omega) = \mathbf{H}_{pri}(\omega)F_{pri}(\omega) + \sum_j \mathbf{H}_{sec,j}(\omega)F_{sec,j}(\omega) \tag{13}$$

where  $F_{pri}(\omega)$  is the primary force acting at  $x = x_{pri}$ ,  $F_{sec,j}(\omega)$  is the  $j^{th}$  secondary force acting at  $x = x_{sec,j}$ ,  $\mathbf{H}_{pri}(\omega) = \{H_1(\omega) \dots H_N(\omega)\}_{pri}^T$  and  $\mathbf{H}_{sec,j}(\omega) = \{H_1(\omega) \dots H_N(\omega)\}_{sec,j}^T$  are the vectors of sensor transfer functions due to primary force  $F_{pri}(\omega)$  and the secondary forces  $F_{sec,j}(\omega)$ , respectively. Substituting Equation (13) into Equation (12) and rearranging yields the feedforward controller transfer function corresponding to the  $j^{th}$  secondary force  $F_{sec,j}(\omega)$ ,

$$H_{con,j} = \frac{F_{sec,j}(\omega)}{F_{pri}(\omega)} = - \left[ \mathbf{Q}_1(\omega), \dots, \mathbf{Q}_j(\omega) \right]^T \cdot \left\{ \mathbf{H}(\omega) \right\}_{sec,j}^{-1} \left[ \mathbf{Q}_1(\omega), \dots, \mathbf{Q}_j(\omega) \right]^T \cdot \left\{ \mathbf{H}(\omega) \right\}_{pri}. \tag{14}$$

Equation (14) implies that at least  $j$  control forces are required to cancel the sound power contributed by the first  $j$  ARMs (Mao & Pietrzko 2013). To implement Equation (14) in time-domain simulations, the estimated value of each frequency-dependent ARM,  $\hat{Q}_{r,n}$ , and sensor transfer functions,  $\hat{H}_n$ , must be used instead. Figure 6 shows the block diagram representation of the feedforward ASAC system. A reference signal is obtained from the disturbance and is used as an input to the digital controller. This controller produces a signal which, when used to drive an appropriate actuation system, is able to reduce the targeted ARM amplitudes, hence reducing the overall radiated sound power.

The controller digital filter is designed using a 65<sup>th</sup> order FIR filter with 32-step delay. It is important to highlight that, the same amount of delay is applied to the disturbance signal to match the timing between both disturbance and controller signals.

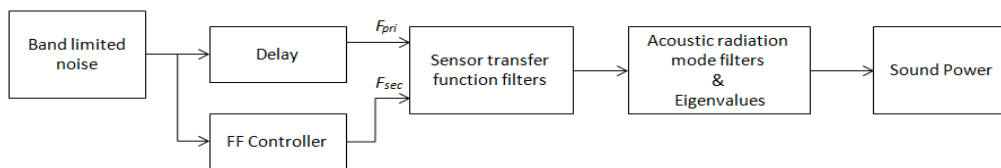


Figure 6: Block diagram representation of the feedforward ASAC

In this simulation, sound power cancelation of the first three ARMs is considered; hence three control forces are required. The locations of the primary force and secondary forces on the beam which controlling the first three ARMs are at  $x_{pri} = 75$  mm,  $x_{sec,1} = 375$  mm,  $x_{sec,2} = 150$  mm and  $x_{sec,3} = 300$  mm, respectively. Figure 7 shows the time domain attenuation of the first three ARM amplitudes when the feedforward controller is turned on at  $t = 5$  seconds. The spectra of the radiated powers can be seen in Figure 8 for different numbers of control forces. Having more modes cancelled will increase the attenuation level as well as its frequency range. Reductions of 9.19 dB, 17.43 dB and 18.17 dB at the beam's first natural frequency of 37 Hz, are achieved by using one control force to cancel the first ARM, two control forces to control the first two ARMs and three control forces to control the first

three ARMs, respectively. For a frequency range of 0 to 400 Hz, the frequency-averaged reduction achieved is about 23 dB when all three control forces are employed. As mentioned in section 2.2, the lower ARM orders have more significant radiation efficiencies, thus cancelling these lower ARM orders will reduce the radiated power considerably.

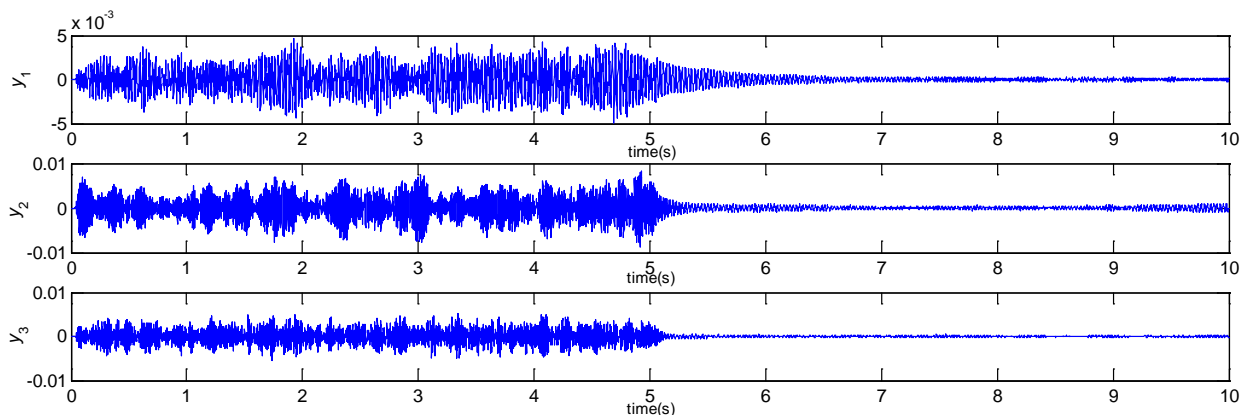


Figure 7: Time histories of the first three ARM amplitudes of beam when the controller is enabled at  $t=5$  seconds

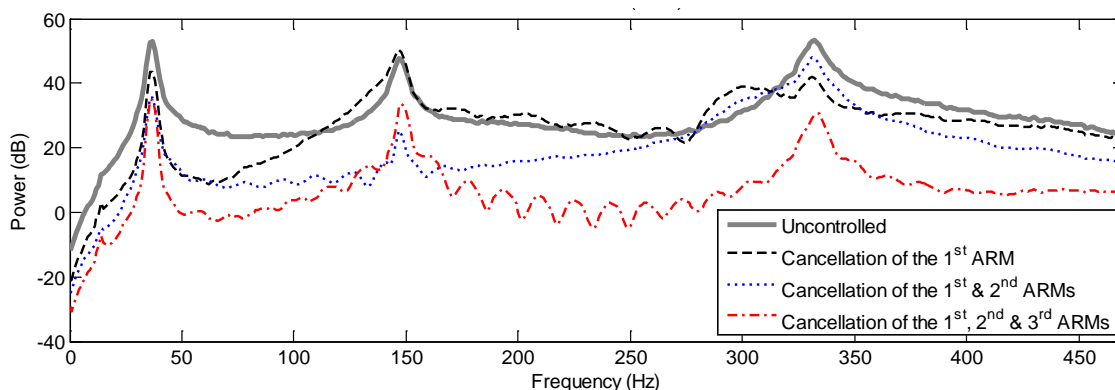


Figure 8: The radiated sound power of vibrating beam

## 6. CONCLUSIONS

In this paper, a method of measuring the radiated sound power from the time-domain estimates of acoustic radiation modes was presented and illustrated by an application to a simply supported beam, although it is applicable to any one-dimensional radiating structure. The ARMs were reconstructed in the time domain using 23<sup>rd</sup> order FIR filters with 11-step delay. These filters were able to fit the ideal frequency responses of ARMs in both magnitude and phase.

To estimate the radiated sound power in the time domain, a Simulink model was created. The resulting ARM filters were used to weight the time series velocities from the vibrating beam and adding them together to produce estimates of the time-domain ARM amplitudes. The radiated sound power was estimated by summing the product of the squares of these ARM amplitudes with the relevant eigenvalues. Simulation results show the frequency response of the radiated sound power estimated using this approach was comparable to the theoretical value.

An active structural acoustic control system was designed using a feedforward control system and real time simulations performed. The proposed digital controllers are able to reduce the targeted ARM amplitudes, hence reducing the overall radiated sound power as well. For the frequency range of interest, i.e. between 0 to 400 Hz, cancellation of the radiated sound power from the first three ARMs was observed. The result shows a frequency-averaged reduction of 23 dB was achieved. This attenuation level can be further improved if the optimal control efforts and its locations were considered.

The benefit of this approach is that it gives broad band control of strongly radiating vibration. It approximates volume velocity control at low frequencies, while conventional ARM control could be designed based on the ARM

shapes at one specific frequency. The advantage of the approach presented here is that the ARM filters allow for the frequency dependence of the ARM shapes, and hence give a better approximation across the frequency range of interest than either of those two methods.

Finally, it is important to highlight that any implementation in this paper is an approximation. Here, large delays/filters were used to explore the potential of the approach. In theory however, fewer filter weights, delays and number of sensors mean fast performance due to less computation time involved but with potentially reduced attenuation. These and other issues are considered elsewhere.

## ACKNOWLEDGEMENTS

The first author would like to acknowledge the Ministry of Higher Education Malaysia (MOHE) and International Islamic University Malaysia (IIUM) for the financial support through SLAB funding. The valuable conference funding from University of Auckland is also appreciated.

## REFERENCES

- Berkhoff, AP 2002, 'Broadband radiation modes: Estimation and active control', *The Journal of the Acoustical Society of America*, vol. 111, no. 3, pp. 1295-305.
- Bianchi, E, Gardonio, P & Elliott, S 2004, 'Smart panel with multiple decentralized units for the control of sound transmission. Part III: control system implementation', *Journal of Sound and Vibration*, vol. 274, no. 1, pp. 215-32.
- Carneal, JP & Fuller, CR 2004, 'An analytical and experimental investigation of active structural acoustic control of noise transmission through double panel systems', *Journal of Sound and Vibration*, vol. 272, no. 3-5, pp. 749-71.
- Choi, S-B 2006, 'Active structural acoustic control of a smart plate featuring piezoelectric actuators', *Journal of Sound and Vibration*, vol. 294, no. 1, pp. 421-9.
- Clark, RL & Fuller, C 1991, 'Control of sound radiation with adaptive structures', *Journal of Intelligent Material Systems and Structures*, vol. 2, no. 3, pp. 431-52.
- Cunefare, KA 1991, 'The minimum multimodal radiation efficiency of baffled finite beams', *The Journal of the Acoustical Society of America*, vol. 90, no. 5, pp. 2521-9.
- Currey, MN & Cunefare, KA 1995, 'The radiation modes of baffled finite plates', *The Journal of the Acoustical Society of America*, vol. 98, no. 3, pp. 1570-80.
- Elliott, SJ 1994, 'Active control of structure-borne noise', *Journal of Sound and Vibration*, vol. 177, no. 5, pp. 651-73.
- Elliott, SJ & Johnson, ME 1993, 'Radiation modes and the active control of sound power', *The Journal of the Acoustical Society of America*, vol. 94, no. 4, pp. 2194-204.
- Elliott, SJ & Nelson, PA 1990, 'The active control of sound', *Electronics & Communication Engineering Journal*, vol. 2, no. 4, pp. 127-36.
- Fuller, CC, Elliott, S & Nelson, PA 1996, *Active control of vibration*, Access Online via Elsevier.
- Gardonio, P, Bianchi, E & Elliott, SJ 2004a, 'Smart panel with multiple decentralized units for the control of sound transmission. Part I: theoretical predictions', *Journal of Sound and Vibration*, vol. 274, no. 1-2, pp. 163-92.
- Gardonio, P, Bianchi, E & Elliott, SJ 2004b, 'Smart panel with multiple decentralized units for the control of sound transmission. Part II: Design of the decentralized control units', *Journal of Sound and Vibration*, vol. 274, no. 1-2, pp. 193-213.
- Gibbs, GP, Clark, RL, Cox, DE & Viperman, JS 2000, 'Radiation modal expansion: Application to active structural acoustic control', *The Journal of the Acoustical Society of America*, vol. 107, no. 1, pp. 332-9.

- Grewal, A, Zimcik, D, Hurtubise, L & Leigh, B 2000, 'Active cabin noise and vibration control for turboprop aircraft using multiple piezoelectric actuators', *Journal of Intelligent Material Systems and Structures*, vol. 11, no. 6, pp. 438-47.
- Johnson, M & Elliott, S 1995, 'Active control of sound radiation using volume velocity cancellation', *The Journal of the Acoustical Society of America*, vol. 98, no. 4, pp. 2174-86.
- Kaizuka, T & Tanaka, N 2008, 'Vibroacoustic modes and active control of both vibration and sound', *AIAA journal*, vol. 46, no. 6, pp. 1490-504.
- Kuo, SM & Morgan, DR 1999, 'Active noise control: a tutorial review', *Proceedings of the IEEE*, vol. 87, no. 6, pp. 943-73.
- Mace, BR & Halkyard, CR 2000, 'Time domain estimation of response and intensity in beams using wave decomposition and reconstruction', *Journal of Sound and Vibration*, vol. 230, no. 3, pp. 561-89.
- Maillard, J 1997, 'Advanced time domain sensing for active structural acoustic control', Virginia Polytechnic Institute and State University.
- Mao, Q & Pietrzko, S 2013, *Control of Noise and Structural Vibration: A MATLAB®-Based Approach*, Springer Science & Business Media.
- Palumbo, D, Cabell, R, Sullivan, B & Cline, J 2001, 'Flight test of active structural acoustic noise control system', *Journal of aircraft*, vol. 38, no. 2, pp. 277-84.
- Pan, J & Bao, C 1998, 'Analytical study of different approaches for active control of sound transmission through double walls', *The Journal of the Acoustical Society of America*, vol. 103, no. 4, pp. 1916-22.
- Pinte, G, Boonen, R, Desmet, W & Sas, P 2009, 'Active structural acoustic control of repetitive impact noise', *Journal of Sound and Vibration*, vol. 319, no. 3-5, pp. 768-94.
- Qiu, J & Ji, H 2010, 'The application of piezoelectric materials in smart structures in China', *International Journal of Aeronautical and Space Science*, vol. 11, no. 4, pp. 266-84.
- Sors, T & Elliott, S 2002, 'Volume velocity estimation with accelerometer arrays for active structural acoustic control', *Journal of Sound and Vibration*, vol. 258, no. 5, pp. 867-83.
- Wu, W 2009, 'Analysis of acoustic radiation mode in time domain', *Science in China Series E: Technological Sciences*, vol. 52, no. 8, pp. 2384-90.